

1 Climatic and hydrologic variability in the East China Sea during the last 7,000 years based on
2 oxygen isotope records of the submarine cavernicolous micro-bivalve *Carditella iejimensis*

3

4 Nagisa Yamamoto^{a*}, Akihisa Kitamura^a, Tomohisa Irino^b, Tomoki Kase^c, Syu-ichi Ohashi^d

5 ^a*Institute of Geosciences, Shizuoka University, Shizuoka 422–8529, Japan*

6 ^b*Faculty of Environmental Earth Science, Hokkaido University, N10W5 Sapporo 060–0810, Japan*

7 ^c*National Science Museum, 3-23-1, Hyakunincho, Shinjyuku-ku, Tokyo 169-0073, Japan*

8 ^d*Kaiyo Planning Co. Ltd., 1732-12, Maeda, Urasoe, Okinawa 901-2102, Japan*

9 * Corresponding author. Tel.: +81 54 238 4798; fax: +81 54 238 0491.

10 *E-mail address: seakita@ipc.shizuoka.ac.jp (A. Kitamura)*

11

Abstract

The micro-bivalve *Carditella iejimensis* inhabits the sediment surface within submarine caves at Ie Island, Okinawa, Japan. A comparison of the $\delta^{18}\text{O}$ values ($\delta^{18}\text{O}_{\text{aragonite}}$) of empty and living shells indicates that the shell is formed over several seasons, and that the main cause of mortality is low water temperature. According to this hypothesis, it is likely that the shells with heaviest $\delta^{18}\text{O}_{\text{aragonite}}$ values (-0.4‰) among the recent dataset formed under or close to the lower limit of growth temperature for the species. Assuming an unchanging temperature tolerance of the species during the Holocene, samples with $\delta^{18}\text{O}_{\text{aragonite}}$ values heavier than -0.4‰ indicate unusually low temperatures and enrichment of $\delta^{18}\text{O}$ of sea water ($\delta^{18}\text{O}_{\text{seawater}}$). The $\delta^{18}\text{O}_{\text{aragonite}}$ record of *C. iejimensis* from sediment cores recovered from Daidokutsu cave shows no clear long-term trend in sea surface temperature or $\delta^{18}\text{O}_{\text{seawater}}$ in the East China Sea during the past 7,000 years, and indicates anomalously cool and dry events (enrichment in $\delta^{18}\text{O}_{\text{seawater}}$) at around 6,300 and 5,550 cal. years BP. These events may have been related to changes in the activity of the East Asian monsoon, related in turn to weakening solar activity. In contrast, these anomalies appear to be obscured during the last 1,000 years, including a weak Asian summer monsoon event during the Little Ice Age, thereby indicating that the mode of the East China Sea climatic and hydrologic response to decadal- to centennial-scale variability in the intensity of East Asian monsoon has varied over the past 7,000 years.

30

Key words: East China Sea, Middle-Late Holocene, submarine cavernicolous micro-bivalve, oxygen isotope, East Asian monsoon

33

34 **1. Introduction**

35

36 The magnitude of natural climate change during the Holocene is one of the key factors in
37 estimating the current and future effects of anthropogenic climate change (e.g., Bond et al., 1997,
38 2001; deMenocal, 2001; Cronin et al., 2003; Mayewski et al., 2004; Wang et al., 2005; Wanner et
39 al., 2008). It is necessary to undertake such studies in many regions of the world, not only because
40 of regional differences in ecosystems and the lifestyle of human populations, but because of spatial
41 variations in the nature and degree of climate change. East Asia, which is home to approximately
42 one-third of the world's population, is strongly influenced by the East Asian monsoon (Fig. 1),
43 which is driven by differential heating between the Asian continent and the surrounding seas and
44 Northwest Pacific.

45 Precisely dated stalagmite oxygen isotope records from southern China reveal that Holocene
46 weakening in the summer monsoon corresponds to an orbitally induced reduction in summertime
47 solar insolation in the Northern Hemisphere (e.g., Dykoski et al., 2005; Wang et al., 2005). On a
48 decadal–century scale, weak Asian summer monsoon events correspond to periods of reduced
49 solar activity (e.g., Neff et al., 2001; Jung et al., 2002; Gupta et al., 2003; Wang et al., 2005).
50 However, Maher (2008) suggested that stalagmite $\delta^{18}\text{O}$ records reflect the declining Holocene
51 influence of isotopically lighter, Indian-monsoon-sourced moisture over China and consequent
52 increase in the proportion of isotopically heavy rainfall, sourced from the relatively oceanic East
53 Asian monsoon. This view was proposed because stalagmite records do not match other East
54 Asian proxy rainfall records based on the magnetic properties of loess/palaeosol (Maher and Hu,
55 2006) and intercomparisons of cave oxygen isotope data (Hu et al., 2008).

56 The winter monsoon has no such signature in the hydrological cycle, and is reconstructed
57 mainly from changes in dust flux. Wang et al. (1999) and Lim et al. (2005) reported that the winter
58 monsoon weakened at 4,000–3,000 years BP in response to increasing winter insolation. Yancheva
59 et al. (2007) claimed that the strengths of the summer and winter monsoons are anti-correlated on a
60 decadal time scale; however, this hypothesis has been challenged by Zhang and Lu (2007) and

61 Zhou et al. (2007). Other studies have argued that centennial-scale variations in the winter
62 monsoon (intensification) are influenced by solar activity (weakening) (Lim et al., 2005; Xiao et
63 al., 2006; Yancheva et al., 2007). Although there is intense debate regarding the nature of Holocene
64 changes in the Asia monsoon, analyses of continental climate records have greatly improved our
65 understanding in this regard. In contrast, few studies have considered the relationship between the
66 East Asian monsoon and the oceanography of the East China Sea, which borders China and Japan.

67 Previous studies have examined Holocene oceanographic changes in the East China Sea based
68 on geochemical analysis of the planktonic foraminifera *Globigerinoides ruber* recovered from
69 deep-sea sedimentary cores (Jian et al., 2000; Ijiri et al., 2005; Sun et al., 2005; Lin et al., 2006).
70 Jian et al. (2000) proposed that a decrease in sea surface temperature (SST) during the period
71 4,600–2,700 cal. years BP was related to an intensification of the winter monsoon. In addition, the
72 authors argued that this decrease in SST may have caused a remarkable decrease in the abundance
73 of the planktonic foraminifera *Pulleniatina obliquiloculata* (i.e., the *Pulleniatina* Minimum Event),
74 which is regarded as the Kuroshio Current indicator species by Jian et al. (1996), Li et al. (1997),
75 and Ujiie and Ujiie (1999). In contrast, Lin et al. (2006) reported no change in SST or sea surface
76 salinity during the *Pulleniatina* Minimum Event. This discrepancy among different studies may
77 reflect the varying quality of data obtained from many different individuals of *G. ruber*.

78 *Globigerinoides ruber* remains at water depths of 2–50 m during its life cycle (Fairbanks et al.,
79 1982; Hemleben et al., 1989; Lin et al., 2004), and thrives in the East China Sea during autumn,
80 spring, and summer when SST is high and the water column is well stratified (Xu et al., 2005).
81 During the summertime development of thermal stratification, sea temperatures vary from
82 28–29°C at 0 m depth to 25°C at 50 m (Xu et al., 2005). Because a single sample for geochemical
83 analysis requires 20–40 individuals of *G. ruber* (Jian et al., 2000; Ijiri et al., 2005; Sun et al., 2005;
84 Lin et al., 2006), each sample represents a mixture of individuals that lived during different years
85 and at different depths.

86 To reconstruct climatic and hydrologic variability in the East China Sea during the Holocene,
87 there exists the need for other long, continuous records of paleoceanographic change. To this end,

88 Kitamura et al. (2007b) and Yamamoto et al. (2008) measured the $\delta^{18}\text{O}_{\text{aragonite}}$ values of empty
89 (dead) and whole shells of the cavernicolous micro-bivalve *C. iejimensis*, which lives in surface
90 sediment within the submarine cave Daidokutsu (meaning *large cave* in Japanese; 29 m water
91 depth; 26°43'N, 127°44'E) of Okinawa, Japan (Fig. 2). Their data reveal that the $\delta^{18}\text{O}$ -derived
92 temperature represents the springtime water temperature for each year, and that there exists no
93 significant millennial-scale trend in the $\delta^{18}\text{O}_{\text{aragonite}}$ record over the past 3,000 years. Because the
94 mixed surface layer was less than 2 cm thick during the deposition of calcareous mud in the cave,
95 time-averaging of the fossil specimens was less than 100 years (Yamamoto et al., 2008). Thus, the
96 $\delta^{18}\text{O}_{\text{aragonite}}$ records of *C. iejimensis* provide unique data for reconstructing Holocene oceanographic
97 changes in the East China Sea. However, Yamamoto et al. (2009b) found no systematic
98 ontogenetic variations in the $\delta^{18}\text{O}_{\text{aragonite}}$ values of empty shells from surface sediment within
99 Daidokutsu cave, which is inconsistent with previous interpretations (Kitamura et al., 2007b;
100 Yamamoto et al., 2008).

101 In the present study, we re-evaluate the potential of $\delta^{18}\text{O}_{\text{aragonite}}$ values of *C. iejimensis* as a tool
102 for reconstructing Holocene oceanographic change. Based on our revised interpretation, we
103 reconstruct climatic and hydrologic variability in the East China Sea during the last 7,000 years
104 based on new data. The results provide information on the evolution of the mode of the climatic
105 and hydrologic response of the East China Sea to the East Asian monsoon.

106

107 **2. Study area and water-temperature conditions**

108

109 The entrances to the submarine caves Daidokutsu and Shodokutsu (meaning *small cave* in
110 Japanese) lie in about 20 m water depth on the fore-reef slope of Ie Island, off the Motobu
111 Peninsula of Okinawa Island (Fig. 2a). Daidokutsu is 40 m long, dark inside, and deepens inward
112 to its deepest point at 29 m below sea level, while Shodokutsu cave is more than 30 m long, dark
113 inside, and has a horizontal cave floor (Fig. 2b and 2c). The floors of both caves are covered by
114 calcareous mud (Hayami and Kase, 1993; Kitamura et al., 2003, 2007a).

115 Kitamura et al. (2007b) and Kitamura and Yamamoto (2009) measured hourly water
116 temperature data in Daidokutsu cave from 26 July 2003 to 6 July 2004, and from 27 August 2007
117 to 19 September 2008 (Fig. 3), revealing seasonal changes from 29°C in August–September to
118 21°C in February. Yamamoto et al. (2009b) reported no significant difference in salinity and
119 $\delta^{18}\text{O}_{\text{seawater}}$ value inside the cave (salinity = 34.3 psu, $\delta^{18}\text{O}_{\text{seawater}} = 0.3 \pm 0.1\text{‰}$) and at 30 m depth
120 outside the cave (salinity = 34.2 psu, $\delta^{18}\text{O}_{\text{seawater}} = 0.4 \pm 0.1\text{‰}$) during early July, which is the
121 summer monsoon season. These data reveal that underground water did not flow into Daidokutsu
122 cave during the observation period and that patterns of seasonal change in water temperature and
123 salinity within the cave are similar to those measured outside the cave at 30 m water depth (mean
124 monthly values) around Okinawa for the period 1906–2003 (Japan Oceanographic Data Center;
125 J-DOSS; $1^\circ \times 1^\circ$ grid cells, 26–27°N latitude and 127–128°E longitude) (Fig. 3a and 3d). We did
126 not measure water conditions in Shodokutsu cave.

127

128 **3. Material**

129

130 *3.1. Shells*

131 *Carditella iejimensis*, which measures less than 3.5 mm in height and length (Fig. 5b), is a
132 shallow infaunal suspension feeder with a shell of 100% aragonite. The species is only found in
133 Daidokutsu and Shodokutsu caves (Fig. 2) among many caves in the Ryukyu Islands, Bonin
134 Islands, Philippine Islands, Saipan, Palau, and Guam (Hayami and Kase, 1993, 1996). No previous
135 study has investigated the ecology of the species. Our preliminary study found only four living
136 specimens in Daidokutsu cave, whereas numerous living specimens were found on the surface
137 sediment within Shodokutsu cave (Hayami and Kase, 1993).

138 Kitamura et al. (2007b) measured the $\delta^{18}\text{O}_{\text{aragonite}}$ values of 30 empty and whole shells of *C.*
139 *iejimensis* picked from the >1 mm fractions of surface sediments (uppermost 5 cm of sediment,
140 representing the past 250 years) within Daidokutsu cave, and obtained a statistically significant
141 correlation between shell size and $\delta^{18}\text{O}_{\text{aragonite}}$ ($r = -0.55$, $p < 0.01$). Yamamoto et al. (2008)

142 added to this dataset the $\delta^{18}\text{O}_{\text{aragonite}}$ values of 17 empty and whole shells collected from surface
 143 sediments within Daidokutsu cave ($n = 47$, $r = -0.37$, $p < 0.05$) (Fig. 5a), and calculated the
 144 following relationship:

$$145 \quad \delta^{18}\text{O}_{\text{aragonite}} = -0.10H - 0.63 \quad (1)$$

146 Using the above equation and the palaeothermometry equation presented by Grossman and Ku
 147 (1986) and Goodwin et al. (2001), we have

$$148 \quad T(^{\circ}\text{C}) = 20.6 - 4.34[\delta^{18}\text{O}_{\text{aragonite/VPDB}} - (\delta^{18}\text{O}_{\text{water/VSMOW}} - 0.2)]. \quad (2)$$

149 Kitamura et al. (2007b) and Yamamoto et al. (2008) estimated the $\delta^{18}\text{O}$ -derived temperature for the
 150 period during the precipitation of small shells (shell height of 1 mm) and the outer portions of
 151 large shells (3.0 mm or more from the umbo), yielding values of 23.8 $^{\circ}\text{C}$ and 26.1 $^{\circ}\text{C}$, respectively.
 152 Given that these values correspond to monthly mean water temperatures during May and July,
 153 respectively, Kitamura et al. (2007b) and Yamamoto et al. (2008) proposed the following
 154 interpretation: the $\delta^{18}\text{O}$ -derived temperature obtained from the shells of *C. iejimensis* indicates
 155 water temperature between May and July of each year. Because the mixed surface layer was less
 156 than 2 cm thick during the deposition of calcareous mud in Daidokutsu cave (thereby indicating
 157 that the time-averaging of the fossil specimens was less than 100 years; Yamamoto et al., 2008),
 158 the $\delta^{18}\text{O}_{\text{aragonite}}$ records of *C. iejimensis* provide high-resolution data for reconstructing
 159 millennial-scale oceanographic change in the East China Sea. A previous analysis of $\delta^{18}\text{O}_{\text{aragonite}}$
 160 values of *C. iejimensis* from three sediment cores from Daidokutsu cave (Cores 02, 04 and 05; Fig.
 161 6) showed no significant millennial-scale trend over the past 3,000 years, suggesting that both
 162 springtime temperature and $\delta^{18}\text{O}_{\text{seawater}}$ at 30 m depth around the Okinawa Islands (Yamamoto et al.,
 163 2008).

164 However, Yamamoto et al. (2009b) found no systematic ontogenetic variations in the
 165 $\delta^{18}\text{O}_{\text{aragonite}}$ values of 19 empty shells, which is inconsistent with previous interpretations that the
 166 $\delta^{18}\text{O}$ -derived temperature obtained from the shells of *C. iejimensis* indicates water temperature
 167 between May and July of each year (Kitamura et al., 2007b; Yamamoto et al., 2008). The authors
 168 proposed that the species may grow over several seasons, but did not speculate on the reason for

169 the size dependence of $\delta^{18}\text{O}_{\text{aragonite}}$ in the empty shells.

170

171 3.2. Cored sediments

172 As noted above, Yamamoto et al. (2008) obtained $\delta^{18}\text{O}_{\text{aragonite}}$ values for *C. iejimensis* over the
173 past 3,000 years, from three sediment cores recovered from Daidokutsu cave. To extend this earlier
174 study, in the present study we collected additional measurements from whole shells within core 19
175 (6 cm in diameter and 233 cm in length), which was collected from Daidokutsu cave during
176 September 2007 (Yamamoto et al., 2009a).

177 The sediment in the core shows a fining-upward trend, and is divided into a lower, gray
178 calcareous sand (233–178 cm depth) and an overlying gray calcareous mud (178–0 cm depth) (Fig.
179 6) (Yamamoto et al., 2009a). Based on ^{14}C age data, the cored sediments preserve a record of
180 fossils and sedimentation over the past 7,000 years. The sedimentation rate is estimated to be 28.6
181 cm/kyr between 233 and 211 cm depth, 49.2 cm/kyr between 211 and 153 cm depth, and 28.9
182 cm/kyr between 153 and 0 cm depth (Fig. 6). Based on temporal changes in the abundance of
183 debris derived from a red soil layer and temporal changes in cavernicolous bivalve assemblages,
184 Yamamoto et al. (2009a) proposed that the filling of cavities within the reefal foundations of the
185 cave has continued over time, resulting in a progressive decrease in the flux of water between the
186 interior and exterior parts of the cave over at least the past 6,500 years.

187

188 4. Methods

189

190 4.1. Water conditions and analysis of $\delta^{18}\text{O}_{\text{seawater}}$

191 We used an Alec Electronics ACT-HR self-registering temperature–salinity meter to measure
192 water temperature and salinity every hour in the innermost part of Shodokutsu cave, from 3 June
193 2007 to 31 July 2009. Unfortunately, records of water temperature within the cave were not
194 obtained between 25 September 2007 and 19 September 2008 due to malfunction of the
195 temperature–salinity meter (Fig. 2c). Water samples for oxygen isotope analysis were collected

196 within Shodokutsu cave and upon the reef slope at 30 m water depth on 2 July 2007.
197 $\delta^{18}\text{O}_{\text{seawater}}$ analyses were performed at the Geo-Science Laboratory in Nagoya, Japan, using a
198 Finnigan MAT delta S. $\delta^{18}\text{O}_{\text{seawater}}$ values are reported relative to VSMOW; analytical precision
199 (1SD) was better than $\pm 0.1\%$.

200

201 4.2. Analyses of $\delta^{18}\text{O}_{\text{aragonite}}$ of micro-shell specimens

202 To examine the cause of the size dependence of $\delta^{18}\text{O}_{\text{aragonite}}$ values for empty shells of *C.*
203 *iejimensis*, we compared $\delta^{18}\text{O}_{\text{aragonite}}$ between living and empty specimens from Shodokutsu cave.
204 For this purpose, samples of 5-cm-thick surface sediment were collected from the middle part of
205 Shodokutsu cave (Fig. 2c) on 3 June 2009 and 29 July 2009.

206 Twenty-nine living individuals and 54 empty specimens of *C. iejimensis* were picked from the
207 >1 mm fractions. We also picked 160 specimens of *C. iejimensis* from the >1 mm fractions of
208 1-cm-thick samples from core 19 (i.e., from 233 sediment samples).

209 All samples received no additional thermal or chemical treatment prior to stable isotope
210 analysis. $\delta^{18}\text{O}_{\text{aragonite}}$ values of whole shells of *C. iejimensis* were determined using a Finnigan
211 MAT 251 mass spectrometer at Hokkaido University, Japan. Individual samples were reacted with
212 100% phosphoric acid at 60°C. Isotope ratios are reported relative to VPDB, and analytical
213 precision (1SD) was better than $\pm 0.08\%$.

214

215 5. Results

216

217 5.1. Water conditions and $\delta^{18}\text{O}_{\text{seawater}}$

218 The results show that water temperature within Shodokutsu cave varied between 20°C and
219 29°C (Fig. 4a). Salinity within the cave showed seasonal change, ranging from 33.5 to 34.5 (Fig.
220 4b). The salinity values from 3 June 2007 to 24 September 2007 are the same as mean monthly
221 salinity measured at 30 m depth in the open sea (J-DOSS, Fig. 4b). On the other hand, the salinity
222 values from October 2008 to July 2009 are 0.4 lower than the mean monthly salinity. For the

223 measurement day (2 July 2007), we found no significant difference in salinity or $\delta^{18}\text{O}_{\text{seawater}}$
 224 between inside the cave (salinity = 33.9 psu, $\delta^{18}\text{O}_{\text{seawater}} = 0.3 \pm 0.1\text{‰}$) and outside the cave at 30 m
 225 depth (salinity = 34.2, $\delta^{18}\text{O}_{\text{seawater}} = 0.4 \pm 0.1\text{‰}$). The obtained $\delta^{18}\text{O}_{\text{seawater}}$ –salinity relationship is
 226 similar to the linear relationship reported by Abe et al. (2009), who measured $\delta^{18}\text{O}_{\text{seawater}}$ and
 227 salinity within surface water at Ishigaki Island (24°20.2'N, 124°9.8'E), Okinawa, Japan, every 10
 228 days from 1998 to 2004 ($\delta^{18}\text{O}_{\text{seawater}} = -10.3 (\pm 0.5) + 0.31 (\pm 0.01) S$, where S = salinity). Based on
 229 the $\delta^{18}\text{O}_{\text{seawater}}$ –salinity relationship and our salinity data, $\delta^{18}\text{O}_{\text{seawater}}$ values within the cave are
 230 estimated to be $0.3 \pm 0.1\text{‰}$ throughout the year.

231 The mean daily temperatures within Shodokutsu cave were higher by $<2^{\circ}\text{C}$ than those in
 232 Daidokutsu cave during summer, while the water temperatures in other seasons were similar
 233 between the caves.

234

235 5.2. $\delta^{18}\text{O}$ values of living and empty specimens from surface sediments

236 The shell heights of living specimens from surface sediments in Shodokutsu cave range from
 237 1.2 to 3.5 mm (Fig. 5b, Table 1). The $\delta^{18}\text{O}_{\text{aragonite}}$ values of living specimens collected in early June
 238 and late July ranged from -1.0 to -1.5‰ and from -1.1 to -1.5‰ , respectively (no significant
 239 difference). There was no significant correlation between shell size and $\delta^{18}\text{O}_{\text{aragonite}}$. The mean and
 240 1σ deviation for $\delta^{18}\text{O}_{\text{aragonite}}$ values were $-1.28 \pm 0.13\text{‰}$.

241 $\delta^{18}\text{O}_{\text{aragonite}}$ values obtained for empty specimens ranged between -1.3 and -0.6‰ , and show a
 242 size dependence ($n = 54$, $r = -0.42$, $p = 0.002$) (Fig. 5c, Table 2). The obtained relationship is as
 243 follows:

$$244 \quad \delta^{18}\text{O}_{\text{aragonite}} = -0.11H - 0.69 \quad (3)$$

245 where H is shell height. The slope of the regression line is similar to that obtained for empty shells
 246 from Daidokutsu cave (-0.10 , Fig. 5a; Yamamoto et al., 2008).

247

248 5.3. $\delta^{18}\text{O}_{\text{aragonite}}$ values of specimens from cored sediments

249 We obtained the $\delta^{18}\text{O}_{\text{aragonite}}$ values of 160 specimens from cored sediments (Table 3).
 250 Kitamura et al. (2007b; core 01) and Yamamoto et al. (2008; cores 02, 04, and 05) reported the
 251 $\delta^{18}\text{O}_{\text{aragonite}}$ values of *C. iejimensis* from cored sediments from Daidokutsu cave. We sorted these
 252 previous data, and our data, into right and left valves (Fig. 7). The $\delta^{18}\text{O}_{\text{aragonite}}$ values range from
 253 -2.1 to 1.7 ‰, with most being between -1.0 and -0.5 ‰ (Fig. 5d). The $\delta^{18}\text{O}_{\text{aragonite}}$ records show
 254 that the long-term trend in $\delta^{18}\text{O}_{\text{aragonite}}$ has been stable for the past 7,000 years, although
 255 anomalously heavy $\delta^{18}\text{O}_{\text{aragonite}}$ values are observed at 6,500 and 5,000 cal. years BP (Fig. 7).

256 We found a statistically significant correlation between $\delta^{18}\text{O}_{\text{aragonite}}$ and shell height for empty
 257 shells from core 19 (Fig. 5d), as follows:

$$258 \quad \delta^{18}\text{O}_{\text{aragonite}} = -0.35H + 0.06 \quad (\text{right valves}) \quad (4)$$

$$259 \quad \delta^{18}\text{O}_{\text{aragonite}} = -0.48H + 0.30 \quad (\text{left valves}) \quad (5)$$

260 The slopes of the regression lines for right and left valves (-0.35 and -0.48 , respectively) are
 261 much steeper than those for empty shells within surface sediments from Daidokutsu and
 262 Shodokutsu caves. Most of the shells with heavy $\delta^{18}\text{O}_{\text{aragonite}}$ values are less than 1.5 mm in height
 263 and are concentrated in periods dated between 6,500 and 5,000 cal. years BP.

264

265 6. Discussions

266

267 6.1. Potential of *C. iejimensis* as an archive of Holocene palaeoceanography

268 There is no significant difference in salinity or $\delta^{18}\text{O}_{\text{seawater}}$ between inside Shodokutsu cave
 269 and outside the cave at 30 m depth, thereby indicating that $\delta^{18}\text{O}_{\text{aragonite}}$ of *C. iejimensis* in the cave
 270 is not influenced by the inflow of underground water.

271 In Shodokutsu cave, the mean water temperature during June is 24.9°C , and about 2°C lower
 272 than values during July (Fig. 4a). Based on the temperature equations for aragonitic molluscan
 273 shells presented by Grossman and Ku (1986) and Carré et al. (2005), a difference in water
 274 temperature of 2°C would cause a 0.5 ‰ variation in the $\delta^{18}\text{O}_{\text{aragonite}}$ value of shell. However, in the
 275 living specimens, there is no significant difference in $\delta^{18}\text{O}_{\text{aragonite}}$ among datasets obtained in early

276 June and late July. Moreover, small individuals are found in late July. These findings are consistent
277 with Yamamoto et al.'s (2009b) hypothesis that the species may be able to grow over several
278 seasons, but are inconsistent with a previous interpretation that shell deposition begins in early
279 April and ends in July (Kitamura et al., 2007b; Yamamoto et al., 2008). We propose that the size
280 dependence of $\delta^{18}\text{O}_{\text{aragonite}}$ of empty shells arises mainly because of the temperature dependence of
281 mortality rate during the juvenile stage.

282 Mortality in bivalves is caused by biotic and abiotic factors. Kase and Hayami (1994)
283 suggested that predators are sparse in Shodokutsu cave and that their activities are infrequent,
284 based on an analysis of the frequency of drilling predation on cavernicolous micro-bivalves.
285 Hayami and Kase (1993) noted that *C. iejimensis* makes up more than 90% of living individuals
286 from the bottom sediments of Shodokutsu cave. In fact, we found several tens of living individuals
287 of the species, but few living individuals of other bivalve species. This dominance of *C. iejimensis*
288 indicates that intraspecific competition, rather than interspecific competition, is the main cause of
289 mortality in the species.

290 The main abiotic agents of mortality are temperature, salinity, oxygen concentration, siltation,
291 and waves (e.g., Dame, 1996). Based on our data and observations, we consider that temperature is
292 the only important abiotic agent of mortality for *C. iejimensis*. Consequently, among all the agents
293 of mortality for this species, we propose that temperature is especially important, and we consider
294 that the size dependence of $\delta^{18}\text{O}_{\text{aragonite}}$ of empty shells of *C. iejimensis* is caused mainly by the
295 high mortality rate of juveniles during exceptionally cold periods. During such periods, the
296 probability of finding a dead immature individual (empty, small shell) within the death assemblage
297 would be much higher than that during periods of normal water temperature. As a result, the
298 proportion of specimens in the death assemblage with high $\delta^{18}\text{O}_{\text{aragonite}}$ would be lower in the
299 subgroup of larger specimens.

300 If the above interpretation is correct, it is likely that shells with the heaviest $\delta^{18}\text{O}_{\text{aragonite}}$ value
301 (-0.4‰) among the recent dataset grew under or close to the lower limit of growth temperature.
302 Many $\delta^{18}\text{O}_{\text{aragonite}}$ values heavier than -0.4‰ are found within sediment deposited between 6,500

303 and 5,000 cal. years BP. Given the widely accepted view that the environmental tolerance of
304 marine invertebrate species is likely to remain largely constant over a period of several thousand
305 years, we consider that the $\delta^{18}\text{O}_{\text{aragonite}}$ values heavier than -0.4‰ indicate unusually low
306 temperature and enrichment of $\delta^{18}\text{O}_{\text{seawater}}$ (dry conditions).

307

308 6.2. Reconstruction of paleoceanographic variations over the past 7,000 years

309 We found no clear long-term trend in the $\delta^{18}\text{O}_{\text{aragonite}}$ records during the last 7,000 years,
310 except for frequent centennial-scale fluctuations. The absence of a long-term trend is consistent
311 with the findings of Sun et al. (2005) and Lin et al. (2006), who estimated SST and $\delta^{18}\text{O}_{\text{seawater}}$
312 based on an analysis of the Mg/Ca and $\delta^{18}\text{O}$ values of the planktonic foraminifera *G. ruber* from
313 deep-sea sediment cores recovered from the East China Sea (Figs. 2 and 6). The authors found no
314 clear insolation-related trend of decreasing intensity in the summer monsoon since the
315 early-middle Holocene, which is characteristic of terrestrial records from monsoon regions (An,
316 2000; Fleitmann et al., 2003; Wang et al., 2005). This observation of a lack of any long-term trends
317 in SST, $\delta^{18}\text{O}_{\text{seawater}}$, or sea surface salinity (SSS) over the past 6,000 years is also supported by
318 other paleoceanographic studies (Ijiri et al., 2005) and simulations of paleoclimate (Kitoh et al.,
319 2006; Oppo et al., 2007). Sun et al. (2005) and Lin et al. (2006) proposed that the absence of
320 long-term trends reflects the complexity of hydrographic processes, as hydrographic conditions
321 were influenced by water originating from both high and low latitudes, which experienced
322 contrasting SST histories during the Holocene. Our study, as well as that of Lin et al. (2006),
323 detected no distinctive, consistent anomalies in the climatic and hydrologic variability associated
324 with the *Pulleniatina* Minimum Event.

325 As noted above, it is likely that $\delta^{18}\text{O}_{\text{aragonite}}$ values heavier than -0.4‰ indicate occurrences of
326 unusually low temperatures and dry conditions. Thus, our records show anomalously cool and dry
327 events at about 6,300 and 5,550 cal. years BP. These events closely coincide with weak Asia
328 summer monsoon events (Neff et al., 2001; Wang et al., 2005; Selvaraj et al., 2007), and the older
329 event corresponds to one of three summertime cold events (which occurred at about 1,700,

330 2,300–4,600, and 6,200 cal. years BP) inferred from the planktonic foraminiferal record of the East
331 China Sea (Xiang et al., 2007). Therefore, we consider that unusually cool and dry events in the
332 East China Sea may have been related to weak summer monsoon events.

333 Abe et al. (2009) detected interannual variation of $\delta^{18}\text{O}_{\text{seawater}}$ of surface water
334 ($+0.007\text{‰}\text{year}^{-1}$) based on continuous records from 1998 to 2004 at Ishigaki Island, and proposed
335 that both a reduction in wintertime northeasterly winds and summertime southwesterly winds
336 caused a decrease in precipitation and consequent enrichment of $\delta^{18}\text{O}_{\text{seawater}}$ around the island. This
337 interpretation is based on the fact that the vapor source for the island is evaporation from the
338 surface of the northern East China Sea in winter and the tropics in summer (Fig. 1). If these
339 processes are applicable to decadal- to centennial-scale variability in the intensity of East Asian
340 monsoon, a weak summer monsoon may result in enrichment of $\delta^{18}\text{O}_{\text{seawater}}$ around the present
341 study area. A strong winter monsoon (anomalously low air temperature) may cause a decrease in
342 $\delta^{18}\text{O}_{\text{seawater}}$ by transporting large amounts of vapor and producing anomalous low SSTs, resulting in
343 heavy $\delta^{18}\text{O}_{\text{aragonite}}$ values. As noted above, although there has been considerable debate regarding
344 the nature of variability in the winter monsoon, Yancheva et al. (2007) reported that the strengths
345 of the winter and summer monsoons are anti-correlated on a decadal time scale. In such a case, a
346 strong winter monsoon may have contributed to the anomalously cool and dry events in the East
347 China Sea at about 6,300 and 5,550 cal. years BP.

348 As noted above, a weak summer monsoon and strong winter monsoon occur during times of
349 weak solar activity (Neff et al., 2001; Fleitmann et al., 2003; Lim et al., 2005; Wang et al., 2005;
350 Xiao et al., 2006; Yancheva et al., 2007). Two anomalously cool and dry events in the East China
351 Sea took place during the interval of Bond event 4, which is an ice-rafting event in the North
352 Atlantic (Bond et al., 2001) (Fig. 7). These findings indicate that these cool and dry events may be
353 related to weak solar activity.

354 It is noteworthy that in the present data, the occurrence of heavy $\delta^{18}\text{O}_{\text{aragonite}}$ values appears to
355 be obscured after 1,000 cal. years BP, even though a weak Asian summer monsoon event occurred
356 during the Little Ice Age (Wang et al., 2005). Sixty $\delta^{18}\text{O}_{\text{aragonite}}$ values fall between 6,500 and 5,500

357 cal. years BP, while 32 values fall in the period between 1,000 years BP and the present. Therefore,
358 it appears to be difficult to explain the absence of anomalously heavy $\delta^{18}\text{O}_{\text{aragonite}}$ values after 1,000
359 cal. years BP in terms of sampling intervals. In addition, Lin et al. (2006) reported that
360 summertime $\delta^{18}\text{O}_{\text{seawater}}$ values in the East China Sea during the early Holocene oscillated between
361 0.7‰ and -0.2‰ , but the magnitudes of the oscillations decreased to $\sim 0.5\text{‰}$ in the middle
362 Holocene and $\sim 0.2\text{‰}$ during 2–1 ka (Fig. 7). These observations may indicate that the mode of the
363 East China Sea climatic and hydrological response to decadal- to centennial-scale variability in the
364 intensity of East Asian monsoon has varied during the past 7,000 years. An examination of the
365 cause of this mode shift is required to further understand natural climate change around the East
366 China Sea and East Asia.

367

368 7. Conclusions

369

370 1. This study found no relationship between shell size and the $\delta^{18}\text{O}_{\text{aragonite}}$ values of living
371 specimens of the submarine cavernicolous micro-bivalve *C. iejimensis*, indicating that the species
372 forms its shell over several seasons. Accordingly, the size dependence of the $\delta^{18}\text{O}_{\text{aragonite}}$ values of
373 empty shells is well explained by the high mortality rate of juveniles during exceptionally cold
374 periods.

375 2. Based on our interpretation that the main cause of mortality in the species is exceptionally
376 low temperature, we consider that the shells that formed at the lower limit of growth temperature
377 represent the heaviest $\delta^{18}\text{O}_{\text{aragonite}}$ values (-0.4‰). It is therefore likely that the $\delta^{18}\text{O}_{\text{aragonite}}$ values
378 heavier than -0.4‰ indicate occurrences of unusually low temperatures and enrichment of
379 $\delta^{18}\text{O}_{\text{seawater}}$ (i.e., dry conditions).

380 3. The obtained $\delta^{18}\text{O}_{\text{aragonite}}$ values indicate no clear long-term trend in SST or $\delta^{18}\text{O}_{\text{seawater}}$ in the
381 East China Sea during the middle–late Holocene, and reveal the occurrence of unusually cool and
382 dry events at around 6,300 and 5,550 cal. years BP. These events were probably related to decadal-
383 to centennial-scale variability in the intensity of the East Asian summer monsoon, which was

384 linked in turn to weakened solar activity.

385 4. The absence of heavy $\delta^{18}\text{O}_{\text{aragonite}}$ values after 1,000 cal. year BP indicates that the mode of
386 the East China Sea climatic and hydrologic response to decadal- to centennial-scale variability in
387 the intensity of East Asian summer monsoon has varied over the past 7,000 years.

388

389 **Acknowledgements**

390 We thank Shigemitsu Kinjo and Koushin Yasumura for collecting samples, and A. Stallard for
391 improving the English in the manuscript. This study was funded by Grants-in-Aid (16340159 and
392 19540492) awarded by the Japan Society for Promotion of Science, The Japan Science Society, a
393 Sasakawa Scientific Research Grant, and a Grant-in-Aid from the Fukada Geological Institute.

394

395 **References**

396 Abe, O., Agata, S., Morimoto, M., Abe, M., Yoshimura, K., Hiyama, T., Yoshida, N., 2009. A 6.5
397 year continuous record of sea surface salinity and seawater isotopic composition at
398 Harbour of Ishigaki Island, southwest Japan. *Isotopes in Environmental and Health Studies*
399 45, 1-12.

400 An, Z.S., Porter, S.C., Kutzbach, J.E., Wu, X.H., Wang, S.M., Liu, X.D., Li, X.Q., Zhou, W.J.,
401 2000. Asynchronous Holocene optimum of the East Asian monsoon. *Quaternary Science*
402 *Reviews* 19, 743-762.

403 Bond, G., Showers, W., Cheseby, M., Lotti, R., Almasi, P., deMenocal, P., Priore, P., Cullen, H.,
404 Hajdas, I., Bonani, G., 1997. A pervasive millennial-scale cycle in the North Atlantic Holocene
405 and glacial climates. *Science* 278, 1257-1266.

406 Bond, G., Kromer, B., Beer, J., Muscheler, R., Evans, M., Showers, W., Hoffmann, S., Lotti-Bond,
407 R., Hajdas, I., Bonani, G., 2001. Persistent solar influence on North Atlantic climate during
408 the Holocene. *Science* 294, 2130-2136.

409 Carré, M., Bentaleb, I., Blamart, D., Ogle, N., Cardenas, F., Zevallos, S., Kalin, R., M., Ortlieb, L.,
410 Fontugne, M., 2005. Stable isotopes and sclerochronology of the bivalve *Mesodesma*

- 411 *donacium*: potential application to Peruvian paleoceanographic reconstructions.
412 Palaeogeography, Palaeoclimatology, Palaeoecology 228, 4-25.
- 413 Cronin, T.M., Dwyer, G.S., Kamiya, T., Schwede S., Willard, D.A., 2003.
414 Medieval warm period, little Ice Age and 20th century temperature variability from
415 Chesapeake Bay. Global and Planetary Change 36, 17-29.
- 416 Dame, R.F., 1996. Ecology of marine bivalves. An ecosystem approach. CRC Press, 254pp.
- 417 deMenocal, P.B., 2001. Cultural responses to climate change during the late Holocene. Science
418 292, 667-673.
- 419 Dykoski, C.A., Edwards, R.L., Cheng, H., Yuan, D., Cai, Y., Zhang, M., Lin, Y., Qing, J., An, Z.,
420 Revenaugh, J., 2005. A high-resolution, absolute-dated Holocene and deglacial Asian
421 monsoon record from Dongge Cave, China. Earth and Planetary Science Letters 233, 71–86.
- 422 Fairbanks, R.C., Sverdrlove, M., Free, R., Wiebe, P.H., Bé, A.W.H., 1982. Vertical distribution and
423 isotopic fractionation of living planktonic foraminifer from the Panama Basin. Nature 298,
424 841-844.
- 425 Fleitmann, D., Burns, S.J., Mudelsee, M., Neff, U., Kramers, J., Mangini, A., Matter, A., 2003.
426 Holocene forcing of the Indian monsoon recorded in a stalagmite from southern Oman.
427 Science 300, 1737-1739.
- 428 Goodwin, D.H., Flessa, K.W., Schöne, B.R., Dettman, D.L., 2001. Cross-calibration of daily
429 growth increments, stable isotope variations, and temperature in the Gulf of California
430 bivalve mollusk *Chione cortezi*: implications for paleoenvironmental analysis. Palaios 16,
431 387-398.
- 432 Grossman, E.L, Ku, T.L., 1986. Oxygen and carbon fractionation in biogenic aragonite:
433 temperature effect. Chemical Geology 59, 59-74.
- 434 Gupta, A.K., Anderson, D.M., Overpeck, J.T., 2003. Abrupt changes in the Asian southwest
435 monsoon during the Holocene and their links to the North Atlantic Ocean. Nature 421,
436 354–357.
- 437 Hayami, I., Kase, T., 1993. Submarine cave bivalvia from the Ryukyu Islands: systematics and

- 438 evolutionary significance. The University Museum, The University of Tokyo, Bulletin 35,
439 1-133.
- 440 Hayami, I., Kase, T., 1996. Characteristics of submarine cave bivalves in the northwestern Pacific.
441 American Malacological Bulletin 12, 59-65.
- 442 Hemleben, C., Spindler, M., Anderson, O.R., 1989. Modern planktonic foraminifera. New York,
443 Springer, 363 p.
- 444 Hu, C., Henderson, G.M., Huang, J., Xie, Sun, Y., Johnson, K.R., 2008. Quantification of Holocene
445 Asian monsoon rainfall from spatially separated cave records. Earth and Planetary Science
446 Letters 266, 221-232.
- 447 Ijiri, A., Wang, L., Oba, T., Kawahata, H., Huang, Chen-Y., Huang, Chi-Y., 2005.
448 Paleoenvironmental changes in the northern area of the East China Sea during the past
449 42,000 years. Palaeogeography, Palaeoclimatology, Palaeoecology 219, 239-261.
- 450 Japan Oceanographic Data Center, Online Data.
451 <http://jdoss1.jodc.go.jp/cgi-bin/1997/bss.jp>
- 452 Jian, Z., Li, B., Pflaumann, U., Wang, P., 1996. Late Holocene cooling event in the western Pacific.
453 Science China, Series, D 39, 543-550.
- 454 Jian, Z., Wang, P., Saito, Y., Wang, J., Pflaumann, U., Oba, T., Cheng, X., 2000. Holocene
455 variability of the Kuroshio Current in the Okinawa Trough, northwestern Pacific Ocean. Earth
456 and Planetary Science Letters 184, 305-319.
- 457 Jung, S.J.A., Davies, G.R., Ganssen, G., Kroon, D., 2002. Decadalcentennial scale monsoon
458 variations in the Arabian Sea during the Early Holocene. Geochemistry Geophysics
459 Geosystems 3, doi 10.10.1029.
- 460 Kase, T., Hayami, I., 1994. Primitiveness of submarine cave mollusks. Fossils 30, 31-36 (in
461 Japanese with English abstract).
- 462 Kitamura, A., Kase, T., Ohashi, S., Hiramoto, M., Sakaguchi, Y., Tanabe, A., Matou, M., 2003.
463 Sedimentary facies and depositional rates of submarine cave sediment in coral reef of
464 Okinawa Islands. The Quaternary Research (Daiyonki-Kenkyu) 42, 99-104 (in Japanese with

- 465 English abstract).
- 466 Kitamura, A., Hiramoto, M., Kase, T., Yamamoto, N., Amemiya, M., Ohashi, S., 2007a. Changes
467 in cavernicolous bivalve assemblages and environments within a submarine cave in Okinawa
468 Islands during the last 5,000 years. *Paleontological Research* 11, 161-180.
- 469 Kitamura, A., Yamamoto, N., 2009. Record of water temperature from 27 August 2007 to 19
470 September 2008 in the submarine cave Daidokutsu, off Ie Island, Okinawa. *Geoscience
471 Reports of Shizuoka University* 36, 31-68.
- 472 Kitamura, A., Yamamoto, N., Kase, T., Ohashi, S., Hiramoto, M., Fukusawa, H., Watanabe, T.,
473 Irino, T., Kojitani, H., Shimamura, M., Kawakami, I., 2007b. Potential of submarine-cave
474 sediments and oxygen isotope composition of cavernicolous micro-bivalve as a late Holocene
475 paleoenvironmental record. *Global and Planetary Change* 55, 301-316.
- 476 Kitoh, A., 2005. Climate model simulation on the role of mountain uplift on Asian monsoon.
477 *Journal of the Geological Society of Japan* 111, 654-667.
- 478 Kitoh, A., Motoi, T., Murakami, J., 2006: El Niño–Southern Oscillation simulation at 6000 years
479 before present with the MRI-CGCM2.3: effect of flux adjustment. *Journal of Climate* 20,
480 2484-2499.
- 481 Li, B., Jian, Z., Wang, P., 1997. *Pulleniatina obliquiloculata* as a paleoceanographic indicator in
482 the southern Okinawa Trough during the last 20,000 years. *Marine Micropaleontology* 32,
483 59-69.
- 484 Lim, J., Matsumoto, E., Kitagawa, H., 2005. Eolian quartz flux variations in Cheju Island, Korea,
485 during the last 6500 yr and a possible Sun-monsoon linkage. *Quaternary Research* 64, 12-20.
- 486 Lin, H.L., Wang, W.C., Hung, G.W., 2004. Seasonal variation of planktonic foraminiferal isotopic
487 composition from sediment traps in the South China Sea. *Marine Micropaleontology* 53,
488 447-460.
- 489 Lin, Y.-S., Wei, K.-Y., Lin, I.-T., Yu, P.-S., Chiang, H.-W., Chen, C.-Y., Shen, C.-C., Mii, H.-S.,
490 Chen, Y.-G., 2006. The Holocene *Pulleniatina* Minimum Event revisited: Geochemical and
491 faunal evidence from the Okinawa Trough and upper reaches of the Kuroshio current. *Marine*

- 492 Micropaleontology 59, 153-170.
- 493 Maher, B.A., 2008. Holocene variability of the East Asian summer monsoon from Chinese cave
494 records: a re-assessment. *The Holocene* 18, 861-866.
- 495 Maher, B.A., Hu, M, 2006. A high resolution record of Holocene rainfall variations from the
496 western Chinese Loess Plateau: antiphase behaviour of the African/Indian and East Asian
497 summer monsoons. *The Holocene* 16, 309-319.
- 498 Mayewski, P.A., Rohling, E.E., Stager J.C, Karlén, W., Maasch, K.A., Meeker, L.D., Meyerson,
499 E.A., Gasse, F., van Kreveld, S., Holmgren, K., Lee-Thorp, J., Rosqvist, G., Rack, F.,
500 Staubwasser, M., Schneider, R.R., Steig, E.J., 2004, Holocene climate variability. *Quaternary*
501 *Research* 62, 243-255.
- 502 Neff, U., Burns, S.J., Mangini, A., Mudelsee, M., Fleitmann, D., Matter, A., 2001. Strong
503 coherence between solar variability and the monsoon in Oman between 9 and 6 kyr ago.
504 *Nature* 411, 290–293.
- 505 Oba, T., 1988. Paleoceanographic information obtained by the isotopic measurement of individual
506 foraminiferal specimens. *Proceedings of the First International Conference on Asian Marine*
507 *Geology*. China Ocean Press, Beijing, p. 169-180.
- 508 Oppo, D.W., Schmidt, G.A., LeGrande, A.N., 2007. Seawater isotope constraints on tropical
509 hydrology during the Holocene. *Geophysical Research Letters* 34, L13701,
510 doi:10.1029/2007GL030017.
- 511 Selvaraj, K., Chen, C. T. A., Lou, J-Y., 2007. Holocene East Asian monsoon variability: Links to
512 solar and tropical Pacific forcing. *Geophysical Research Letters* 34, L01703,
513 doi:10.1029/2006GL028155.
- 514 Sun, Y., Oppo D.W., Xiang, R., Liu, W., Gao, S., 2005. Last deglaciation in the Okinawa Trough:
515 Subtropical northwest Pacific link to Northern Hemisphere and tropical climate.
516 *Paleoceanography* 20, PA4005, doi:10.1029/2004PA001061.
- 517 Ujiie, H., Ujiie, Y., 1999. Late Quaternary course changes of the Kuroshio Current in the Ryukyu
518 Arc region, northwestern Pacific Ocean. *Marine Micropaleontology*, 37, 23-40.

- 519 Wang, L., Sarnthein, M., Erlenkeuser, H., Grimalt, J., Grootes, P., Heilig, S., Ivanova, E., Kienast,
520 M., Pelejero, C., Pflaumann, U., 1999. East Asian monsoon climate during the Late
521 Pleistocene: high-resolution sediment records from the South China Sea. *Marine Geology* 156,
522 245-284.
- 523 Wang, Y., Cheng, H., Edwards, L., He, Y., Kong, X., An, Z., Wu, J., Kelly, M.J., Dykoski, C.A., Li,
524 X., 2005. The Holocene Asian monsoon: links to solar changes and North Atlantic climate.
525 *Science* 308, 854-857.
- 526 Wanner, H., Beer, J., Bütikofer, J., Crowley, T. J., Cubasch, U., Flückiger, J., Goosse, H., Grosjean,
527 M., Joos, F., Kaplan, J.O., Küttel, M., Müller, S.A., Prentice, C., Solomina, O., Stocker, T.F.,
528 Tarasov, P., Wagner M., Widmann, M., 2008. Mid- to Late Holocene climate change: an
529 overview. *Quaternary Science Reviews* 27, 1791-1828.
- 530 Xiang, R., Sun, Y., Li, T., Oppo, D.W., Chen, M., Zheng, F., 2007. Paleoenvironmental change in
531 the middle Okinawa Trough since the last deglaciation: Evidence from the sedimentation rate
532 and planktonic foraminiferal record. *Palaeogeography, Palaeoclimatology, Palaeoecology* 243,
533 378-393.
- 534 Xiao, S., Li, A., Liu, J.P., Chen, M., Xie, Q., Jiang, F., Li, T., Xiang, R., Chen, Z., 2006. Coherence
535 between solar activity and the East Asian winter monsoon variability in the past 8000 years
536 from Yangtze River-derived mud in the East China Sea. *Palaeogeography, Palaeoclimatology,*
537 *Palaeoecology* 237, 293-304.
- 538 Xu, X., Yamasaki, M., Oda, M., Honda, C.M., 2005. Comparison of seasonal flux variations of
539 planktonic foraminifera in sediment traps on both sides of the Ryukyu Islands, Japan. *Marine*
540 *Micropaleontology* 58, 45-55.
- 541 Yamamoto, N., Kitamura, A., Irino, T., Kase, T., Ohashi, S., 2008. Reconstruction of
542 paleotemperatures in Northwest Pacific over the past 3,000 years from $\delta^{18}\text{O}$ values of the
543 micro-bivalvia *Carditella iejimensis* found in a submarine cave. *Global and Planetary Change*
544 62, 97-106.
- 545 Yamamoto, N., Kitamura, A., Ohmori, A., Morishima, Y., Toyofuku, T. and Ohashi, S., 2009a.

- 546 Long-term changes in sediment type and cavernicolous bivalve assemblages in Daidokutsu
547 submarine cave, Okinawa Islands: evidence from a new core extending over the past 7,000
548 years. *Coral Reefs* 28, 967–976.
- 549 Yamamoto, N., Sakai S., Kitamura, A., 2009b. Evaluation of the $\delta^{18}\text{O}$ value of the submarine
550 cavernicolous micro-bivalve *Carditella iejimensis* as a proxy for palaeotemperature.
551 *Paleontological Research* 13, 279-284.
- 552 Yancheva, G., Nowaczyk, N.R., Mingram, J., Dulski, P., Schettler, G., Negendank, J.F.W., Liu, J.,
553 Sigman, D.M., Peterson, L.C., Haug, G.H., 2007. Influence of the intertropical convergence
554 zone on the East Asian monsoon. *Nature* 445, 74-77.
- 555 Zhang, D., Lu, L., 2007. Anti-correlation of summer/winter monsoons? *Nature* 450, E7-E8.
- 556 Zhou, H., Guan, H., Chi, B., 2007. Record of winter monsoon strength. *Nature* 450, E10-E11.
- 557

558 Figure Captions

559

560 Figure 1 Spatial distributions of observed mean surface wind (vectors) in East Asia for the periods
561 June–August and December–February. Modified from Kitoh (2005).

562

563 Figure 2 (a) Location maps of Daidokutsu and Shodokutsu submarine caves at Ie Island, off
564 Okinawa Japan, the locations of drill cores A7 (Sun et al., 2005; Xiang et al., 2007) and MD403
565 (Lin et al., 2006), and Dongge cave, China. NEC: North Equatorial Current; KC: Kuroshio Current.
566 (b) Simplified cross-section of Daidokutsu cave, showing the location of core sample 19. (c)
567 Simplified cross-section of Shodokutsu cave.

568

569 Figure 3 Observed temperatures within Daidokutsu cave. The observation period was from 26 July
570 2003 to 6 July 2004, and from 27 August 2007 to 19 September 2008.

571

572 Figure 4 (a) Observed temperatures within Shodokutsu cave. The observation period was from 3
573 June 2007 to 24 September 2007 and from 20 September 2008 to 31 July 2009. (b) Observed
574 salinities within Shodokutsu cave. The observation period was from 3 June 2007 to 24 September
575 2007 and from 20 September 2008 to 31 July 2009. Seasonal variations in salinity (monthly mean
576 values) at 30 m depth for the period 1906–2003 ($1^{\circ} \times 1^{\circ}$ grid cells; $26\text{--}27^{\circ}\text{N}$ latitude and
577 $127\text{--}128^{\circ}\text{E}$ longitude). Error bars represent one standard deviation (1σ).

578

579 Figure 5 Relationship between $\delta^{18}\text{O}$ and the shell height of *C. iejimensis*. Error bars represent one
580 standard deviation of a single $\delta^{18}\text{O}$ analysis. Note that the vertical axes are inverted so that higher
581 temperatures (lower $\delta^{18}\text{O}$) are toward the top. (a) Empty shells from surface sediment within
582 Daidokutsu cave; (b) living shells from surface sediment within Shodokutsu cave; (c) empty shells
583 from surface sediment within Shodokutsu cave; (d) empty shells from core 19 within Daidokutsu
584 cave.

585

586 Figure 6 Stratigraphic columns compiled for cores 01, 02, 04, 05, and 19 recovered from within
587 Daidokutsu cave, showing the stratigraphic distribution of Daidokutsu pumice. Also shown is a
588 map of the distribution of surface sediment facies within the cave. Facies 1, gray calcareous sand;
589 Facies 2, gray calcareous mud; Facies 3, calcareous sand containing the skeletons of partly
590 encrusted coralline sponges.

591

592 Figure 7 Comparison of $\delta^{18}\text{O}$ values of *C. iejimensis* from cored samples (present day) with the
593 $\delta^{18}\text{O}_{\text{seawater}}$ record from the East China Sea (Lin et al., 2006), stalagmite $\delta^{18}\text{O}$ record from Dongge
594 cave in southeast China (Wang et al., 2005), and record of ice-rafted debris from the North Atlantic
595 (Bond et al., 2001). Note that the axes are inverted so that higher temperatures (lower $\delta^{18}\text{O}$) are
596 toward the top.

597

598 Table 1 Results of oxygen isotope analyses of living specimens of *C. iejimensis* from Shodokutsu
599 cave.

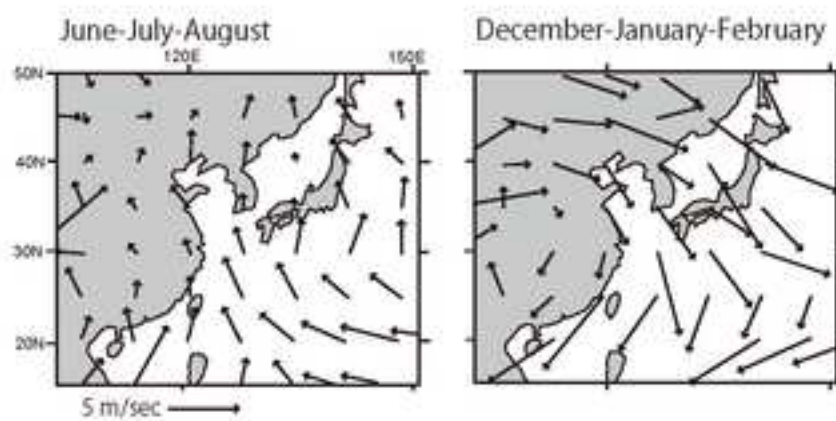
600

601 Table 2 Results of oxygen isotope analyses of empty specimens of *C. iejimensis* from surface
602 sediments in Shodokutsu cave.

603

604 Table 3 Results of oxygen isotope analyses of empty specimens of *C. iejimensis* from core 19 in
605 Daidokutsu cave.

Figure 1
[Click here to download high resolution image](#)



Yamamoto et al Fig. 1

Figure 2

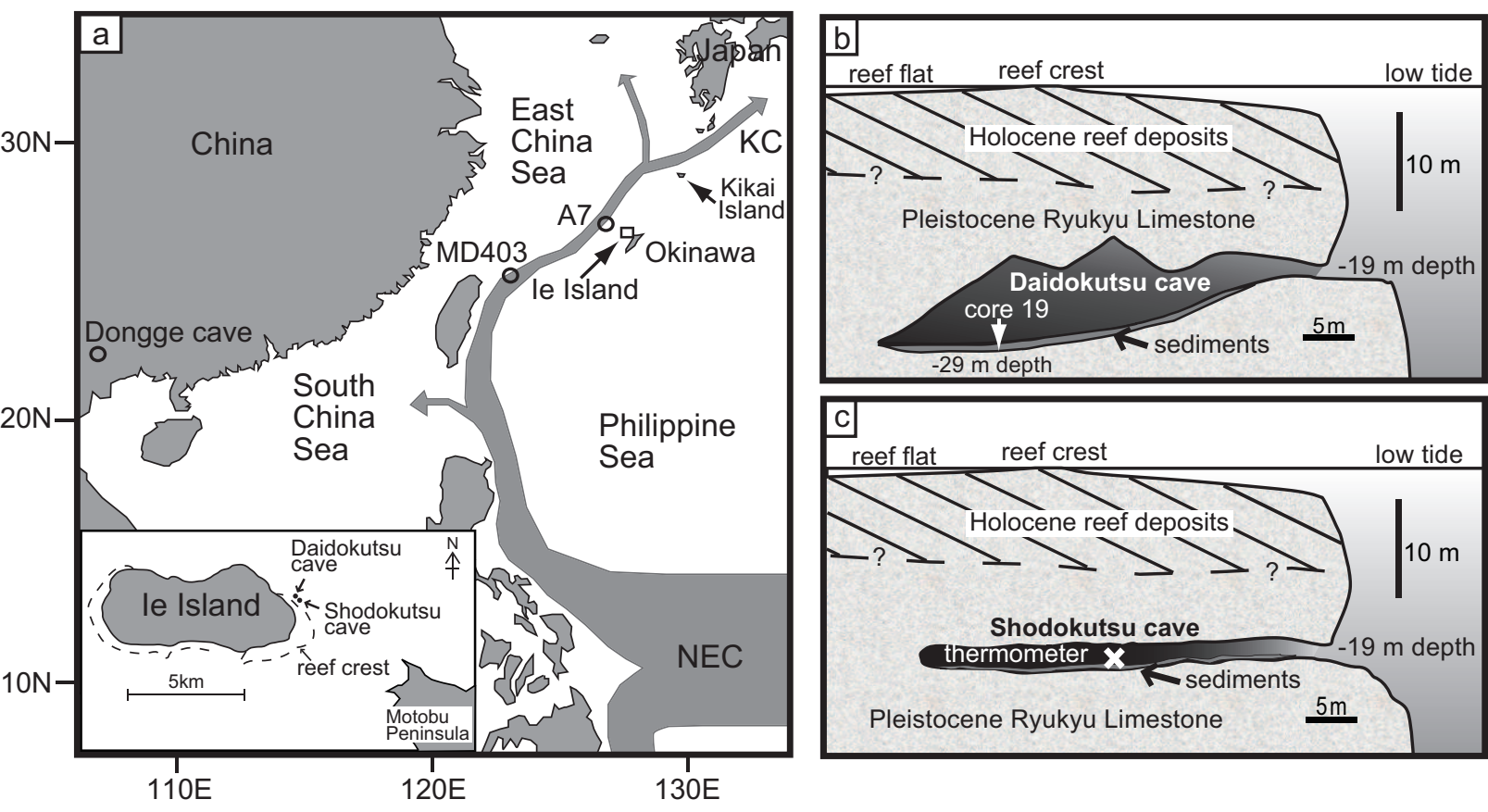
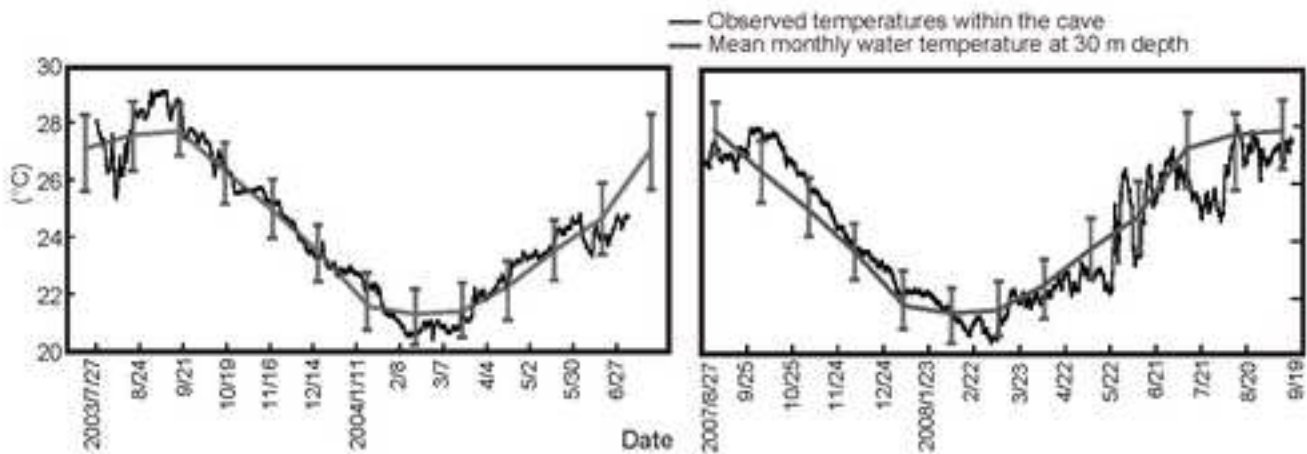
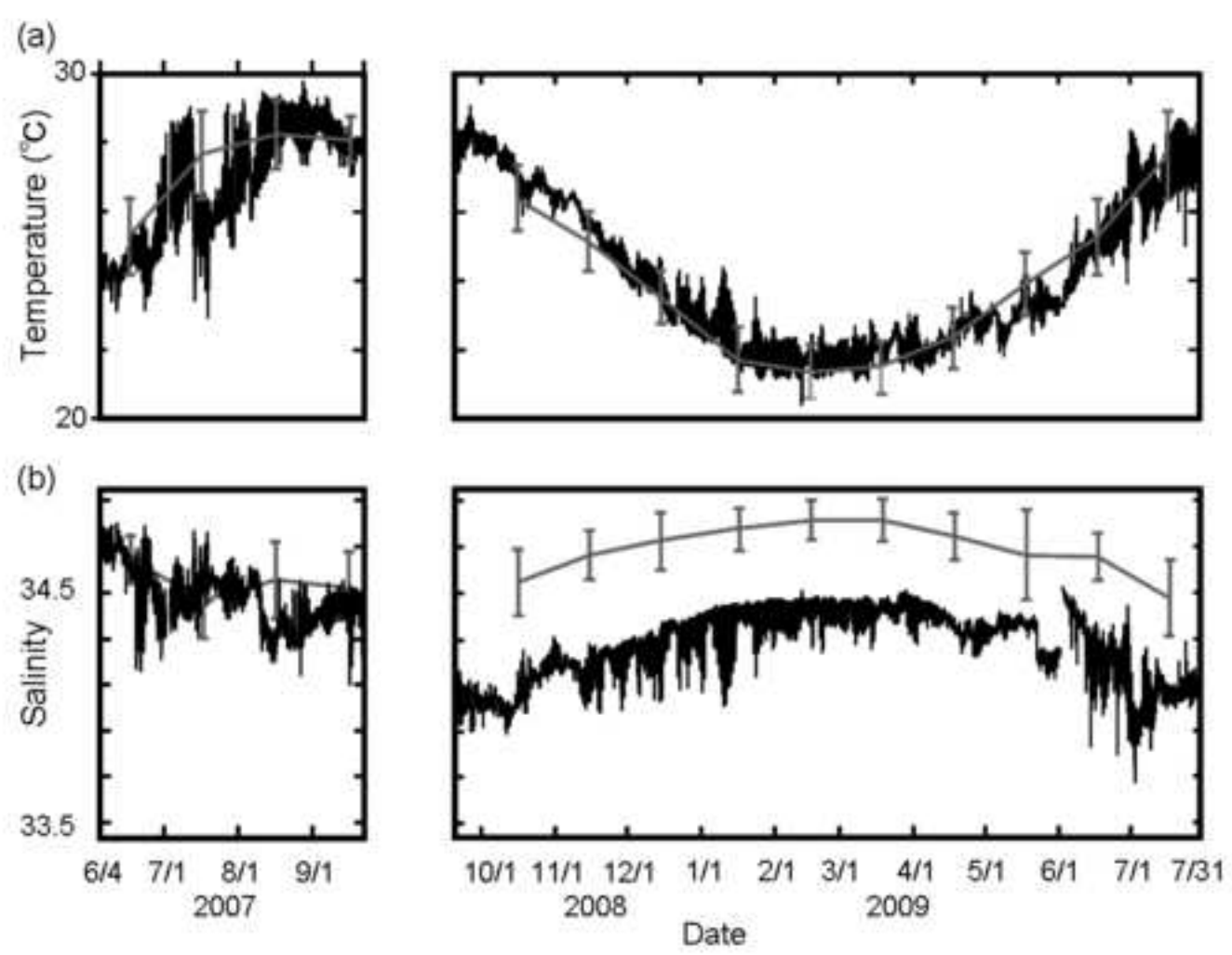


Figure 3
[Click here to download high resolution image](#)



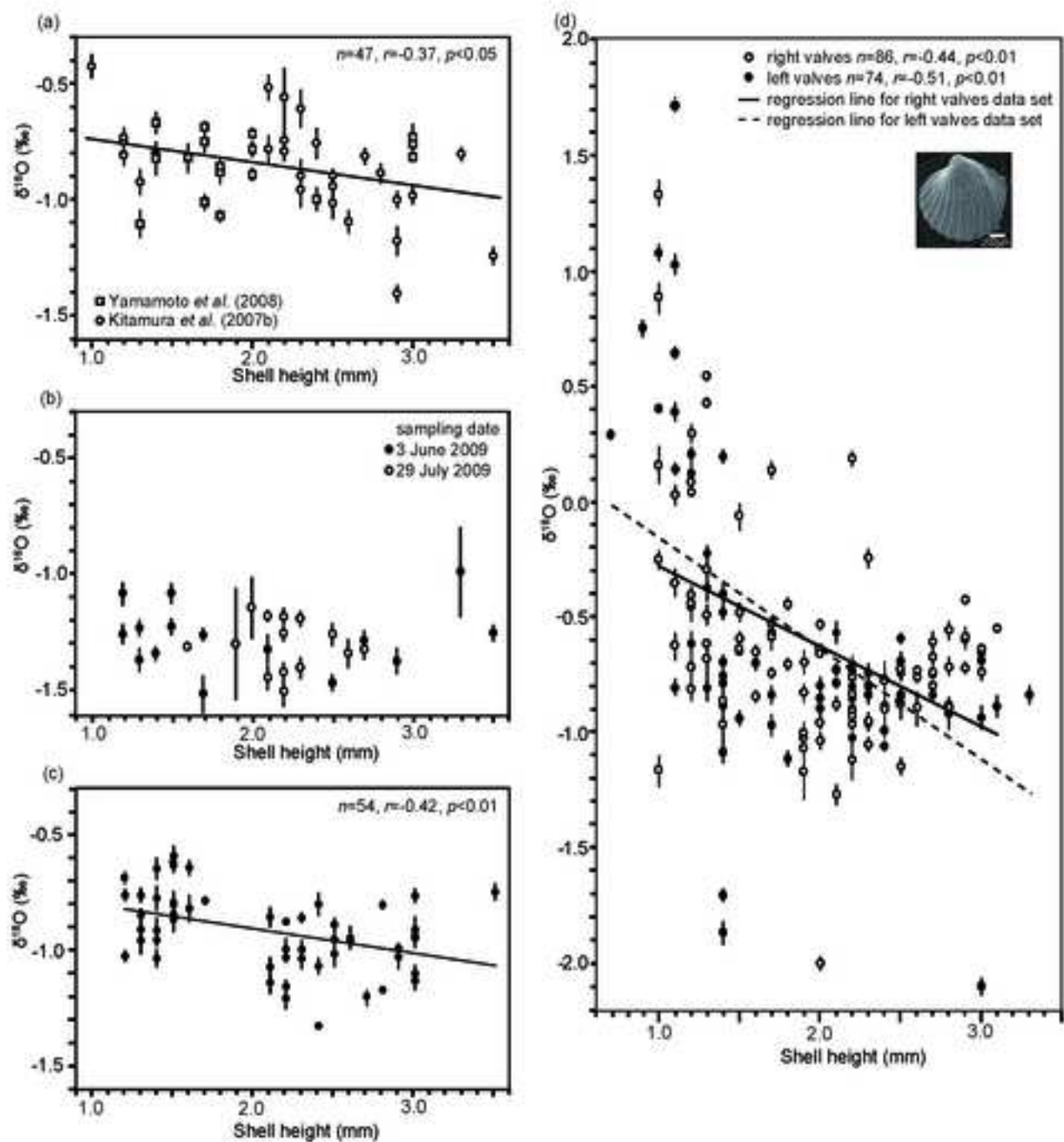
Yamamoto et al Fig. 3

Figure 4
[Click here to download high resolution image](#)



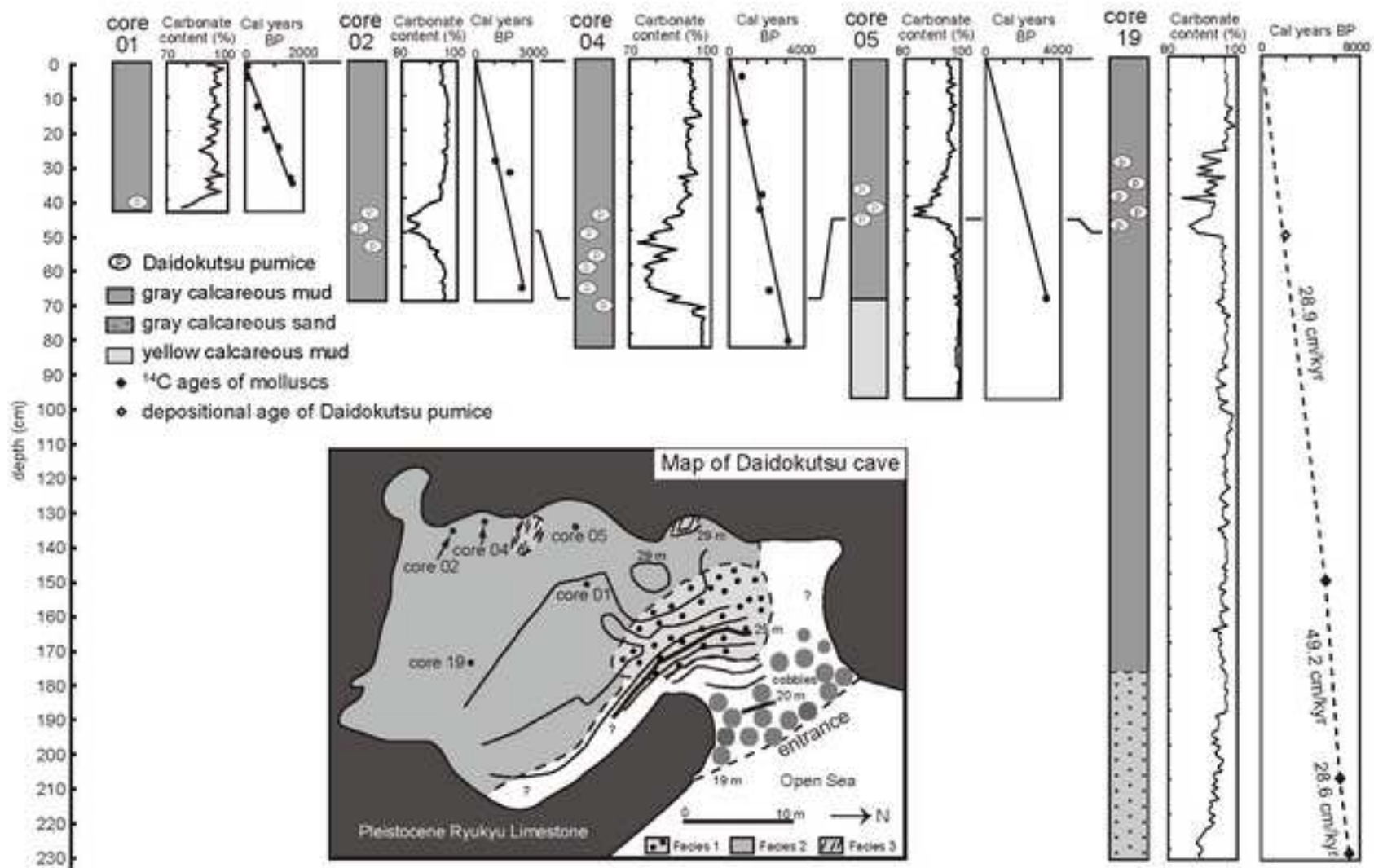
Yamamoto et al. Fig. 4

Figure 5
[Click here to download high resolution image](#)



Yamamoto et al Fig. 5

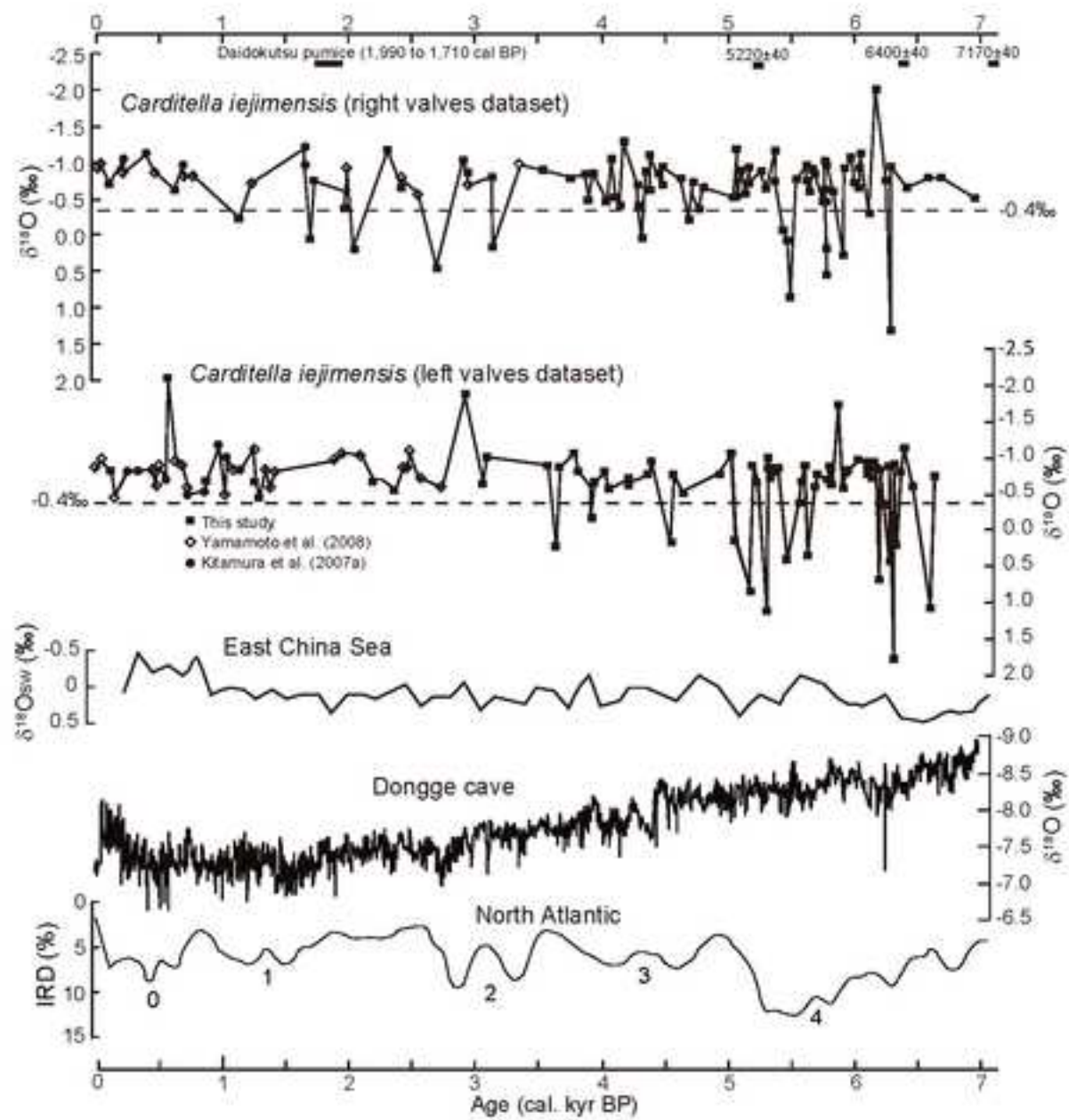
Figure 6
[Click here to download high resolution image](#)



Yamamoto et al. Fig 6

Figure 7

[Click here to download high resolution image](#)



Yamamoto et al Fig. 7

Table 1

collected in 2009/6/3		collected in 2009/7/29	
Height (mm)	$\delta^{18}\text{O}$	Height (mm)	$\delta^{18}\text{O}$
3.5	-1.25	2.7	-1.32
3.3	-0.98	2.6	-1.33
2.9	-1.37	2.5	-1.25
2.7	-1.28	2.3	-1.40
2.5	-1.46	2.3	-1.18
2.1	-1.31	2.2	-1.50
1.7	-1.51	2.2	-1.41
1.7	-1.25	2.2	-1.25
1.5	-1.22	2.2	-1.17
1.5	-1.08	2.1	-1.44
1.4	-1.34	2.1	-1.17
1.3	-1.36	2.0	-1.14
1.3	-1.22	1.9	-1.29
1.2	-1.25	1.6	-1.30
1.2	-1.08		

Yamamoto et al. Table 1

Table 2

Height (mm)	$\delta^{18}\text{O}$	Height (mm)	$\delta^{18}\text{O}$
1.2	-1.02	2.2	-1.16
1.2	-0.76	2.2	-1.03
1.2	-0.69	2.2	-0.99
1.3	-0.96	2.2	-0.88
1.3	-0.91	2.3	-1.03
1.3	-0.85	2.3	-1.00
1.3	-0.76	2.3	-0.86
1.4	-1.03	2.4	-1.33
1.4	-0.95	2.4	-1.07
1.4	-0.91	2.4	-0.80
1.4	-0.91	2.5	-1.01
1.4	-0.77	2.5	-0.95
1.4	-0.65	2.5	-0.90
1.5	-0.87	2.6	-0.96
1.5	-0.84	2.6	-0.95
1.5	-0.80	2.7	-1.20
1.5	-0.79	2.8	-1.17
1.5	-0.63	2.8	-0.80
1.5	-0.62	2.9	-1.03
1.5	-0.59	2.9	-0.99
1.6	-0.82	3.0	-1.13
1.6	-0.64	3.0	-1.10
1.7	-0.78	3.0	-0.95
2.1	-1.14	3.0	-0.93
2.1	-1.07	3.0	-0.91
2.1	-0.85	3.0	-0.76
2.2	-1.21	3.5	-0.75

Yamamoto et al. Table 2

Table 3

Depth (cm)	Valve	Height (mm)	$\delta^{18}\text{O}$	Depth (cm)	Valve	Height (mm)	$\delta^{18}\text{O}$	Depth (cm)	Valve	Height (mm)	$\delta^{18}\text{O}$	Depth (cm)	Valve	Height (mm)	$\delta^{18}\text{O}$
3.5	R	2.5	-0.73	118.5	R	1.9	-1.02	154.5	R	2.1	-0.88	185.5	L	2.5	-0.59
4.5	L	3.3	-0.84	119.5	R	2.9	-0.59	155.5	L	1.0	1.08	186.5	L	1.1	-0.80
17.5	L	3.0	-2.10	120.5	R	1.8	-0.44	156.5	R	1.1	-0.63	186.5	R	1.2	0.30
18.5	R	2.0	-0.64	121.5	R	2.1	-1.27	156.5	L	1.7	-0.84	187.5	R	2.5	-0.88
26.5	L	3.0	-0.69	122.5	L	2.8	-0.71	156.5	L	2.4	-0.99	188.5	L	2.5	-0.84
33.5	R	2.3	-0.24	122.5	L	3.0	-0.65	157.5	L	1.4	-0.69	189.5	R	2.3	-1.05
37.5	L	2.5	-0.74	124.5	R	1.3	-0.68	158.5	L	1.3	-0.81	190.5	R	1.8	-0.70
38.5	L	1.4	-0.48	124.5	R	2.9	-0.42	158.5	L	1.4	-0.87	190.5	R	2.6	-0.73
49.5	R	1.1	0.03	125.5	R	1.2	0.04	159.5	R	2.5	-1.14	191.5	L	1.7	-0.97
50.5	R	2.7	-0.75	126.5	R	1.4	-0.86	159.5	R	2.8	-0.72	192.5	R	1.6	-0.65
57.5	R	1.2	-0.40	126.5	R	2.7	-0.61	160.5	L	2.7	-0.83	192.5	R	2.8	-0.89
59.5	R	1.0	0.16	127.5	R	1.9	-1.07	162.5	R	1.5	-0.06	193.5	R	2.2	-1.12
64.5	L	2.2	-0.73	127.5	L	2.3	-0.79	163.5	L	1.1	0.39	194.5	L	1.4	-0.78
67.5	R	1.9	-1.17	127.5	R	3.0	-0.64	164.5	R	1.2	0.08	194.5	L	1.5	-0.94
69.5	L	2.9	-0.59	128.5	L	3.0	-0.93	165.5	R	1.0	0.89	195.5	L	2.5	-0.84
70.5	R	2.7	-0.67	130.5	R	1.9	-0.69	167.5	R	2.6	-0.76	196.5	R	1.3	-0.29
78.5	R	1.3	0.43	130.5	R	2.3	-0.95	168.5	L	1.4	-0.40	196.5	L	2.3	-0.74
84.5	R	2.0	-1.03	132.5	L	1.1	0.15	169.5	L	1.6	-0.70	197.5	L	2.3	-0.96
85.5	L	1.4	-1.86	133.5	L	2.1	-0.78	170.5	L	2.2	-0.89	198.5	L	2.0	-0.85
85.5	R	2.5	-0.87	134.5	R	2.4	-0.77	171.5	L	0.7	0.29	199.5	L	1.1	0.65
89.5	L	2.5	-0.69	135.5	L	2.1	-0.56	171.5	R	2.2	-0.97	199.5	R	2.0	-2.00
90.5	R	1.2	-0.81	136.5	R	1.0	-0.25	171.5	R	2.7	-0.74	200.5	L	2.3	-0.80
90.5	L	2.2	-1.02	137.5	R	1.2	-0.72	172.5	R	1.7	-0.59	201.5	L	1.3	-0.37
91.5	R	1.7	0.14	137.5	R	3.0	-0.74	173.5	R	2.4	-0.90	202.5	R	1.7	-0.74
103.5	R	2.6	-0.90	137.5	R	3.1	-0.55	174.5	L	1.2	-0.61	203.5	L	1.0	0.40
104.5	L	2.8	-0.91	138.5	R	1.1	-0.35	174.5	R	2.2	-0.83	203.5	L	2.2	-0.85
106.5	L	1.2	0.21	139.5	R	2.0	-0.66	175.5	L	1.4	-0.75	204.5	R	1.0	1.34
107.5	L	3.1	-0.89	143.5	L	2.0	-0.79	177.5	R	1.2	-0.45	204.5	R	2.2	-0.93
109.5	R	2.7	-0.80	146.5	R	1.7	-0.53	178.5	R	1.3	-0.62	205.5	L	1.1	1.72
110.5	L	1.4	-1.08	146.5	L	2.4	-1.06	178.5	R	1.4	-0.97	205.5	L	1.4	-0.88
111.5	L	2.3	-0.84	147.5	R	1.0	-1.17	178.5	R	1.9	-1.00	206.5	L	1.4	0.20
112.5	R	1.9	-0.82	147.5	L	1.2	0.12	179.5	L	1.2	-0.71	208.5	L	2.2	-0.80
113.5	R	2.0	-0.53	147.5	R	2.8	-0.56	179.5	R	1.2	-0.44	209.5	L	1.8	-1.11
114.5	L	1.2	-0.61	148.5	R	2.4	-0.88	179.5	R	1.3	0.54	210.5	R	1.5	-0.64
114.5	L	1.3	-0.22	149.5	R	1.7	-0.57	179.5	R	2.0	-0.96	212.5	L	1.5	-0.63
114.5	R	1.6	-0.84	150.5	L	0.9	0.75	179.5	R	2.2	0.19	215.5	R	2.2	-0.76
115.5	L	2.2	-0.71	150.5	R	2.2	-0.91	180.5	L	2.8	-0.88	216.5	L	1.1	1.03
117.5	L	1.4	-0.79	150.5	R	2.9	-0.71	181.5	L	1.5	-0.65	217.5	L	2.1	-0.72
117.5	R	1.5	-0.48	151.5	L	2.0	-0.90	181.5	R	1.5	-0.60	218.5	R	2.4	-0.77
118.5	L	1.7	-0.59	152.5	L	2.7	-0.67	183.5	L	1.4	-1.70	226.5	R	1.3	-0.49

Yamamoto et al. Table 3